Assessment of tumour glucose uptake using gluco-CEST

S. Walker-Samuel[1], P. Johnson[2], B. Pedley[2], M. F. Lythgoe*[1], and X. Golay*[3]
[1]UCL Centre for Advanced Biomedical Imaging, Department of Medicine and Institute of Child Health, University College London, London, United Kingdom, [2]Institute of Cancer, University College London, United Kingdom, [3]Institute of Neurology, University College London, United Kingdom

* Joint senior authors

Introduction

Tumours typically exhibit a greater reliance on glycolytic metabolism than normal tissues due to hypoxia and/or inhibited mitochondrial function [1,2]. This upregulated glucose metabolism is exploited by PET with the use of ^{18}F fluorodeoxyglucose (FDG), which is routinely used for tumour detection in the clinic. Similarly, ^{13}C-labelled 2-deoxy-D-glucose has been used to measure glucose metabolism *in vivo*, albeit with modest sensitivity [3]. It has been shown that glycogen can be detected in the liver with MRI through the use of chemical exchange saturation transfer (CEST), via the exchange of saturated protons in $^{-}$OH groups with those in bulk tissue water [4]. The aim of this study was to determine whether, using a similar approach, the accumulation of exogenously administered glucose could be detected in tumour xenograft models. Two acquisition sequences were used to evaluate the effect: one with a spatially selective spectroscopic readout (EXPRESS), which allows the confounding influence of fat on CEST data to be corrected [5,6], and the other with a gradient echo imaging readout, which enabled the spatial distribution of glucose enhancement to be evaluated.

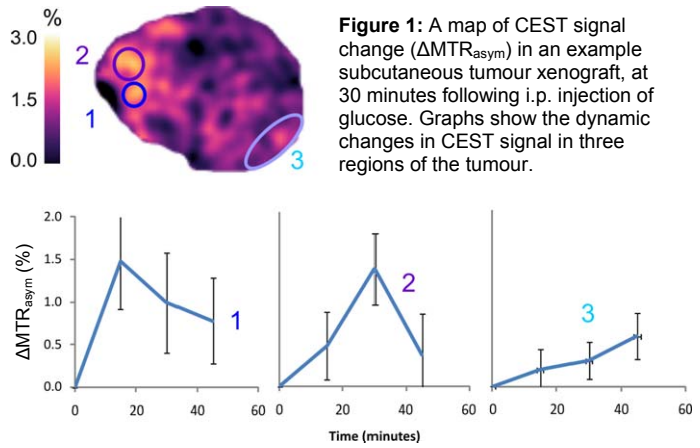

Figure 1: A map of CEST signal change (ΔMTR_{asym}) in an example subcutaneous tumour xenograft, at 30 minutes following i.p. injection of glucose. Graphs show the dynamic changes in CEST signal in three regions of the tumour.

Methods and Materials

SW1222 subcutaneous colorectal tumour xenograft models (MF1 nude mice, n=6), with an average tumour volume of 1.9 ± 0.4 cm^3 following 15 days of growth, were scanned using a 9.4T Varian scanner and a 39mm birdcage coil (Rapid MR International, Columbus, Ohio). Mice were anaesthetised using isoflurane in air, and either cannulated via a tail vein or an intra-peritoneal line. During scanning, core body temperature was monitored and maintained at 37° using a warm air blower. Following shimming, CEST data were acquired using two sequences, the first based on a localised spectroscopic readout (EXchange modulated Point-REsolved Spatially Selective (EXPRESS) [5,6], seq.1) and the other a spoiled gradient echo sequence (seq.2). For both, selective saturation was induced using a train of 100, 6 ms Gaussian pulses, each separated by a 2 ms delay (effective bandwidth 50 Hz). Frequency offsets of between -3500 and +3500 Hz were applied, at 50 Hz intervals, in addition to reference data at a frequency offset of 80,000 Hz. Sequence 1 acquired data from a voxel encompassing the entire tumour (TR=6s, TE=12 ms, voxel size ~2 cm^3), whereas data from sequence 2 consisted of a single slice positioned in the centre of the tumour (TR=3.5 ms, TE=1.2 ms, flip angle = 13°, slice thickness = 1 mm, matrix size = 128×128, FOV = 3.5×3.5 cm^2).

Following acquisition of a set of baseline scans, 0.2 g/kg of glucose solution was injected either intravenously (i.v.) or intraperitoneally (i.p.). Between two and six interleaved sets of data from seq. 1 and 2 were then acquired dynamically for 60 to 120 minutes post-injection. Static field offsets were corrected by spline fitting of z-spectra and shifting the lowest intensity point to 0 ppm. Whole-tumour MTR_{asym} spectra were calculated from data from seq.1, using the following relationship [7]: $MTR_{asym} = (S^- - S^+) / S_{ref}$, where S^- and S^+ are data acquired during saturation offsets on opposite sides of the water resonance; S_{ref} is the reference measurement at 80,000 Hz. MTR_{asym} spectra were also calculated on a pixel-by-pixel basis for data from seq.2.

Enhancement due to glucose uptake was evaluated by integrating EXPRESS MTR_{asym} spectra between -0.5 and -3.0 ppm (to emcompass the $^{-}$OH resonance between -0.5 and -1.5 ppm [4]) and subtracting the baseline measurement from post-glucose injection measurements (ΔMTR_{asym}, expressed as a percentage). Dynamic glucose uptake data were fitted with a bi-exponential function of the form $\Delta MTR_{asym} = S_0 (1 - e^{-r1.t})e^{-r2.t}$.

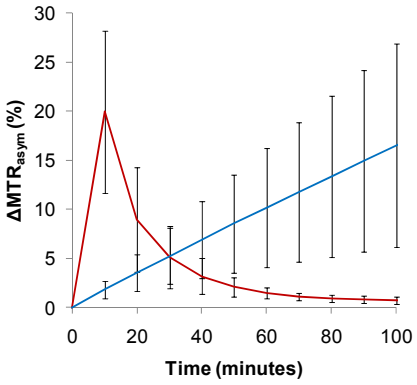

Figure 2: Aggregated glucose enhancement curves for i.v. (red) and i.p. (blue) injection, taken from model fits to individual whole-tumour uptake curves.

Results and Discussion

Figure 1 shows a map of CEST signal change (ΔMTR_{asym}) in an example tumour, calculated from data acquired with seq.2, which demonstrates typical glucose enhancement patterns observed *in vivo*. Measured glucose uptake within the tumour was heterogeneous, which may have been mediated by pH and hypoxic state variations within the tumour. Evaluation of whole tumour data acquired with seq.1 (shown in Fig. 2) revealed that i.v. and i.p. glucose injections resulted in different uptake curves, with i.v. kinetics showing rapid washin and clearance and i.p. injections showing a longer, slower enhancement (r_1 = 0.02 ± 0.01 /min (i.p.) and 164 ± 24 /min (i.v.); r_2 = 0.12 ± 0.07 /min (i.v.)). All but one tumour demonstrated a significant increase in ΔMTR_{asym} at one or more time points following the baseline scan ($p<0.01$, Wilcoxon rank sum).

Conclusion

The results of this pilot study are the first to demonstrate that the uptake of exogeneously administered glucose by tumours can be detected using CEST MRI. The technique was sensitive enough to detect regional differences in tumour uptake and differences in injection route. Further work is being undertaken to fully quantify the effect, including the influence of pH on proton exchange rates and to evaluate the basis of the observed regional heterogeneity.

Acknowledgements

King's College London and UCL Comprehensive Cancer Imaging Centre, CR-UK & EPSRC, in association with the MRC and DoH (England), and the British Heart Foundation.

References

[1] Carew, JS & Huang, P, Molecular Cancer, 2002, 1:9 [2] Vaupel, P, Cancer Metastasis Rev, 2007;26(2):225-239 [3] Kotyk, JJ *et al.*, J Neurochem, 1989;53:1620-8. [4] Van Zijl, PCM *et al*, PNAS, 2007;107(44):4359-4364 [5] Walker-Samuel, S *et al*, Proc. British Chapter of the ISMRM, 2010 [6] Walker-Samuel, S *et al*, Proc. ISMRM 2011 [7] Zhou, J *et al*, Magn Reson Med, 2003; 50(6):1120-1126.